# Optimization of A Patch-Based Approach to Finger Vein Verification with a Convolutional Neural Network

Tugce Arican
Computer Science, University of Twente
Supervised by Raymond Veldhuis and Luuk Spreeuwers

***Abstract*—Finger veins are accepted as unique for each person, and since finger veins are below the skin, they are more resistant to forgery. In this paper, a patch-based approach using a convolutional neural network is explored. The patch-based approach increases the number of labeled data, and helps against brightness variations, yet, at the same time, it introduces its own issues such as determining the patch properties, combining the patches, and registration of the image pairs. This research proposes an optimisation to the patch based finger vein verification approach by addressing these issues. The patch-based system has achieved 0.3% of equal error rate and 0.999 area under the curve on UTFVP and 6.6% of equal error rate and 0.969 area under the curve on SDUMLA-HMT after proposed optimisations. Even though the results are far from the state-of-the-art performance, the improvement indicates the potential of the proposed system.**

## I. Introduction

Vascular patterns are unique for each person; therefore, they could be used in human identification. Finger vein pattern is one of the vascular patterns, and it has some advantages over other biometrics. Since they are below the skin, it is more difficult to forge them compared o face or finger prints. Moreover, finger vein patterns are more resistant to external factors such as aging or scars.

An identification system using vascular patterns could perform image verification by comparing a probe image with a registered one. If a matching score computed in this comparison exceeds a threshold, the identity is verified, rejected otherwise. Images belonging to the same subject are called as genuine pairs. If they belong to different subjects, then the pairs are said to be imposter.

Several approaches have been proposed to design a finger vein human identification system. Conventional methods mainly utilise manually extracted features and matching distance. Line tracking [1], or cross-sectional areas [2], [3] have been proposed to extract the vein pattern. Gabor filters [4], Local Binary Patterns(LBP) [5] are also used as textural features. Beside the whole vein pattern or textural information, end or bifurcation points [28], [29] are also used. Personalised Best Patch Map(PBPM) [33] and localised sub-regions [34] are also proposed to finger vein verification to achieve a system robust to partial-distortions. Conventional methods achieve high recognition accuracy; however, since they are based on manually extracted features, these approaches could be tailored to the dataset or the problem itself.

There is a growing body of literature that recognises Machine learning based approaches in finger vein verification. These approaches rely on machine learning methods, such as neural networks, fuzzy logic, for the final decision. Wu and Liu showed machine learning based approaches could achieve high accuracy in finger vein pattern identification by using Support Vector Machines(SVM) [26] and Adaptive Neuro Fuzzy System(ANFIS) [25].

As a machine learning approach, Convolutional Neural Networks(CNNs) are proposed in finger vein human identification. [8], [14], [15], and [16] have achieved promising recognition rates indicating the potential of the CNN based approaches. [17] proposed to use difference image rather than the whole image in order to reduce the complexity of the CNN. Different than the previous ones [35] used a CNN to extract the finger vein structure by assigning labels for pixels as foreground and background.

A patch-based approach using a CNN has been proposed by [11] aiming to achieve a robust finger vein verification system to brightness variations. Rather than scoring the whole image, the network is fed by small square regions, called patches. After scoring, the individual patch scores are combined to an image score for the final decision. The proposed method achieved promising results showing the feasibility of the patch based approach with a CNN. A diagram of the system is shown in Figure1.

However, the patch-based approach in [11] has some issues which could prevent the approach from achieving its optimal. First of all, the use of patch properties such as patch size, shape, and overlapping were not investigated. It is likely that an improper patch could degrade the performance by dividing junctions unintentionally. Secondly, in [11], two fusion methods were explored under uniformity assumption. As not all the patches involve the same information, the uniformity assumption may not reflect the expected results. Finally, the effects of displacements on x-axis on the registration accuracy was not examined. The coarse registration used in [11] uses finger edges for image registration, and it could fail since these kind of displacements do not change the finger edges much. This paper, proposes solutions to these issues

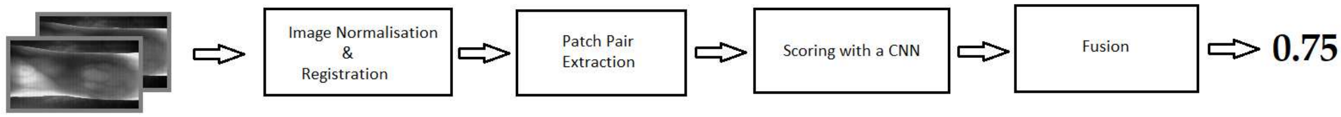


Fig. 1: Block diagram of the system

by investigating different patch sizes and shapes, also the overlapping patches. Moreover, the fusion method considering the differences among patches, and the registration approach which could consider the displacement in the x-axis have been implemented.

Considering the literature and the existing system this work investigates the following cases.

*Research Question 1:* What is the proper patch size and shape for the existing system?

*Research Question 2:* How could overlapping patches influence the verification?

*Research Question 3:* How could the contribution of each patch be determined with a computationally less complex fusion method?

*Research Question 4:* How could the displacements, which are ignored by the existing registration method, be taken into account?

This paper is organized as follows. Chapter II gives a brief overview about what has been done about finger vein biometrics until now. Chapter III explains the patch-based finger verification system in a detailed way and the methods used in this paper. Chapter IV presents the results achieved. Chapter V discusses the findings. Finally, Chapter VI closes this paper with a conclusion and future work.

## II. Related Work

Various studies have indicated the patch-based approaches could benefit in solving several issues. For instance, [20] applied a patch based approach aiming to reduce the computational complexity of cancer image classification with a CNN. Since the input image has very high resolution, e.g. gigapixels, these patches help to reduce the resolution of the input, therefore the complexity of the CNN. Moreover, the patch based approach allowed to select only the relevant patches. [35] applied the patch-based CNN approach to extract finger vein patterns from raw images. The patches are centered on pixels. Then, a CNN assigns a probability of being a foreground pixel to the corresponding patch. The authors were able to achieve significant improvements on two public dataset in terms of finger vein verification accuracy. [11] utilised a patch-based CNN to finger vein verification aiming to achieve more robust verification system to brightness changes. The results achieved indicates the feasibility of the patch-based CNN approach to finger vein verification.

While they provide many opportunities, the patch properties are crucial for the patch-based approaches. [36] proposed a patch-based approach with Collaborative Representation based Classification(CRC) to face recognition in aiming to increase training samples, and different patch sizes have been investigated in this research. The obtained results indicated that the recognition performance is dependent on the selected patch size. [37] argued that not only the patch size but also the shape of the patch affect the performance. The authors proposed to use superpixels instead of fixed shape patches. The results achieved showed the importance of the selected patch shape. Overlapping patches approach used in [36], [22], and [21] achieved promising improvements indicating that overlapping patches could provide improvements on the performance.

In patch-based systems, the patches are scored individually, therefore, these scores must be fused to an image score. Since each patch could carry different information, a fusion operation should consider these differences. However, such a fusion is computationally expensive. [10] showed such a fusion is possible with less computational complexity. The authors applied a patch-based approach to face recognition aiming to achieve a robust system to brightness variations and facial expressions. They proposed a fusion method which determines a threshold for each patch by using only one parameter, called False Acceptance Rate (FAR) value. The FAR value is set at the beginning, and it is assumed that patches having poor scores could not contribute much to the final score since the FAR value will set a high threshold for those patches. The promising results they achieved in face recognition indicate the feasibility of the proposed approach.

In a patch-based approach, patch pairs are extracted according to their relative locations. Therefore, image registration has an influence on the overall performance. Registration is generally done based on the physical properties, e.g. edges, or reference points, e.g. landmarks. [30] and [13] showed that a better registration accuracy is possible with a matching score based approach. In [30], a performance metric computed from face recognition similarity scores were attempted to be maximized among a set of alignment candidate. One of the alignment candidates reaching the maximum performance metric has been selected as the aligned image. Similarly, [13] used an iterative method for image registration utilising a matching score based approach. The authors searched a set of geometric translations. One of the geometric translations minimising the matching score has been accepted as the registration parameters.

## III. The Existing System and Methodology

### A. Patch-based Finger Vein Verification

The finger vein verification system proposed by [11] consists of 5 steps, namely image registration, patch extraction,

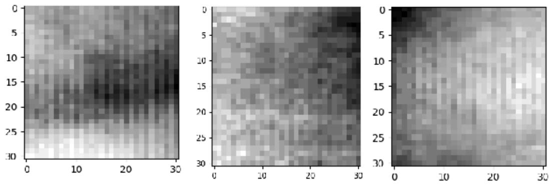

Fig. 2: 31-pixel patch samples from UTFVP

scoring, fusion, and decision. Figure 1 indicates the block diagram of the existing system.

Image pairs are registered based on utilising Iterative Closest Point (ICP) [12] algorithm. ICP uses the finger edges in order to align two finger vein images. Later, the center line of the finger images is used to correct the orientation of the fingers. After registration, 31 pixels square patch pairs are extracted only from the finger region. A CNN is fed by these patch pairs, and outputs a matching score for each. These patch pair scores are fused to an image score. [11] compared two fusion methods namely decision and score level fusions. Finally, the fused scores are compared against a threshold for the final decision.

### B. Methodology

The following section describes the proposed solutions to the issues found in the existing systems and explains how to apply them.

*1) Patch Size:* In [11], it is stated that the maximum width of finger veins are approximately 20 pixels. Therefore, a vein might occupy a large area in a 31 pixels patch such that the network could not learn much from it. Visual inspection of the patches revealed that veins are ambiguous or not visible in 31 x 31 patches (Figure 2). In this research, the larger patch sizes than 31-pixel were investigated. The patch sizes were selected as 49, 57, 63, 69, 75, 82, and 88 pixels.

The patches were extracted in the same way described in [11]. Only the size used to extract patches was changed.

*2) Patch Shape:* Finger veins lay horizontally. Thus, square patch shape might not be the optimal choice for the proposed system. Rectangular patches could capture the horizontal vein structure better than square ones. The height of the patch was fixed to the best performing patch size. Table I presents the patch widths used in experiments.

The patches were extracted in the same way described in [11]. Only the width used to extract patches was changed.

| Dataset | Patch Width (px) | | | |
|---|---|---|---|---|
| UTFVP | 123 | 164 | 205 | 226 |
| SDUMLA-HMT | 104 | 139 | 174 | 209 |

TABLE I: Patch widths used in the experiments

*3) Overlapping:* Overlapping patches are another aspect of patch-based systems. Overlapping patches could help to catch some vein structures which cannot be seen with non-overlapping patches. Moreover, the overlapping increases the number of labelled data by providing more variations about the veins, which helps the network to learn the vein structures better.

The overlapping patches were extracted in the same way described in [11], except a smaller stride than the patch size has been used in both height and width. The smaller stride leads more overlap, hence more similarity among adjacent patches. The strides used are presented in Experiment 3.

*4) Fixed-Far Voting Fusion:* A non-uniform voting fusion method is formulated in equations 1 and 2. $LR_i$ defines the score of the system *i*, while $T_i$ denotes the individual threshold for the system *i*. $V_i$ votes are collected by comparing the score of each system against its threshold.

$$V_i = \begin{cases} 0 & , LR_i < T_i \\ 1 & , LR_i \geq T_i \end{cases} \tag{1}$$

After collecting all $V_i$ votes, a score *S* is computed as a sum of these votes, as shown in 2. This *S* score is compared to a threshold *T* to form a final decision. However, determining the $T_i$ values for each system individually is computationally expensive.

$$D = \begin{cases} \text{reject, } S = \sum_i V_i < T \\ \text{accept, } S = \sum_i V_i \geq T \end{cases} \tag{2}$$

Fixed-Far Voting Fusion(FFVF) proposed by Spreeuwers et.al. [10] aimed to simplify the determination of the individual threshold $T_i$. The authors proposed to set a False Acceptance Rate(FAR) value for each system in order to determine the individual thresholds. It was assumed that poor systems would not be able to cast votes often since their FAR value determines their threshold as high.

In this research, each patch was considered as an individual system. By setting a FAR value, an individual threshold was computed for each patch.

*5) Fine Registration:* A fine registration step has been implemented based on the idea of minimising/maximising an objective proposed by Spreeuwers et.al. [13]. The objective in this research was determined as maximizing the output of the network, aka. matching score. Different alignment candidates have been generated by applying a shift operation within a range of values on the object pair. Then, each pair has been scored, and the candidate pair having the maximum matching score has been selected as the registered pair. Figure 3 shows the steps involved in fine registration.

Two implementations have been done by utilising the proposed matching score based approach.

*a) Local Fine Registration:* The shift operation has been applied on individual patch pairs. The object patch was shifted up to 4 pixels in 8 directions, namely up, down, left, right, and their combinations. Since the displacements were in the patch level, the small range of shift values has been selected.

*b) Global Fine Registration:* The shift operation has been applied on the object image. The whole image was shifted in 8 directions, namely up,down, left, right, an their combinations. In the global level, larger displacements were

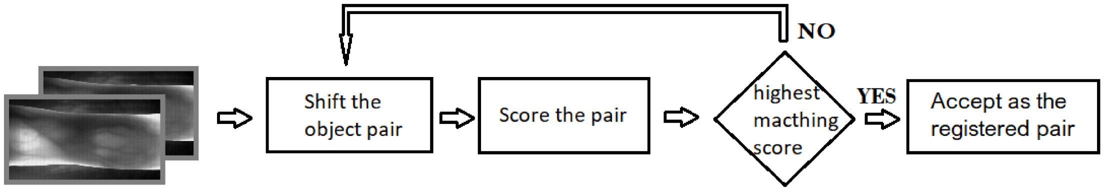


Fig. 3: Steps involved in fine registration

considered. Therefore, shift range has been determined as 40 pixels.

## IV. Experiments and Results

In this section, five experiments were conducted to demonstrate the performance of the proposed solutions. The first three experiments have been done to find optimal patch properties namely patch size, patch shape, and overlapping stride. The fourth experiment was executed to investigate the feasibility of Fixed-FAR voting fusion on the patch based finger vein verification. In the last experiment, the performance of the proposed fine registration method was examined.

In all experiments, except Experiment 3, the datasets more or less have the same size, approximately 190000 patch pairs. Since the changes in patch size and shape affect the number of patches extracted, some overlap was applied to keep the dataset sizes stable.

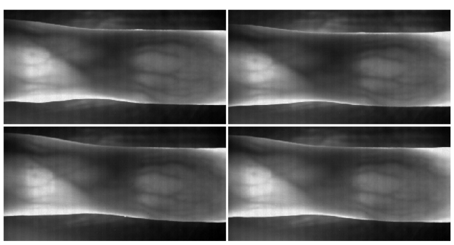

Fig. 4: Sample finger vein images from UTFVP

The network was trained with the appropriate settings for each experiment. For instance, if en evaluation is done with 82-pixel patches, the training is also done with the 82-pixel patch size. Only UTFVP dataset was used to train the network due to its higher quality.

The performance of the system was evaluated by Equal Error Rate (EER) and FRR@FAR=0.1%. EER is measured where False Reject Rate (FRR) is equal to False Acceptance Rate (FAR).

### A. Databases

In this work, 2 different databases from two universities, which are explained below, were used to evaluate the proposed optimisation solutions.

*1) University of Twente:* UTFVP [9] consists of 1440 finger vein images from 60 subjects. In total, 24 finger vein images were captured from each subject, which consists of total 6 fingers from 2 hands e.g., index, middle, and ring fingers. The fingers were illuminated above by 8 near infrared LEDs. The LEDs had been adaptively controlled for more uniform intensity. Some samples can be seen in Figure 4.

The finger vein images were saved in 8-bit gray scale png files with a resolution of 672x380 pixels. Image capturing was done in two sessions.

*2) Shandung Univesity:* SDUMLA-HMT [27] was developed by Shandung University. It is a muti-modal biometrics database which consists of face, iris, finger vein, and gait images. The finger vein database composes 3,816 finger vein images from 106 persons. 6 images were captured for each of the 6 fingers from 2 hands e.g. index, middle and ring fingers. Figure 5 shows some samples from the database.

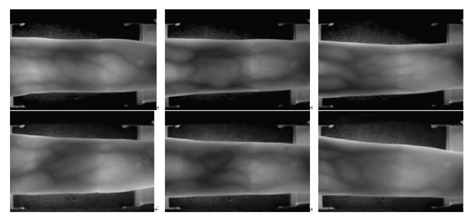

Fig. 5: Sample finger vein images from SDUMLA-HMT

The finger vein images were saved as 8 bit rgb format in bmp files. Resolution of the images are 320x240 pixels. No guide bar was used during capturing the images, and no session information was given.

### B. Experiment 1 - Patch Size

The aim of this experiment was to optimise the size of the patches.The patch sizes selected as 49, 57, 63, 69, 75, 82, and 88 pixels. A subset of 10 subjects was selected from UTFVP was used. This dataset involves 2160 finger vein image pairs (720 genuine, 1440 imposter). All 106 subjects in SDUMLA-HMT database were used in the experiments. This dataset involves 57240 image pairs in total (19080 genuine, 38160 imposter).

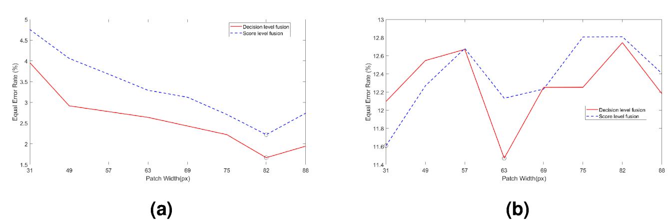


Fig. 6: EER for varying values of patch sizes (a) UTFVP, (b) SDUMLA-HMT

Figure 6a shows a decrease in EER on UTFVP with the larger patch sizes. Table II presents the performance of

31-pixel and 82-pixel patches. 82-pixel patches performed significantly better than 31-pixels. The larger patch involves more vein structure, therefore, the network could find better matches. Figure 7 supports this claim. The larger patch led a better score distribution compared to 31-pixel patches.

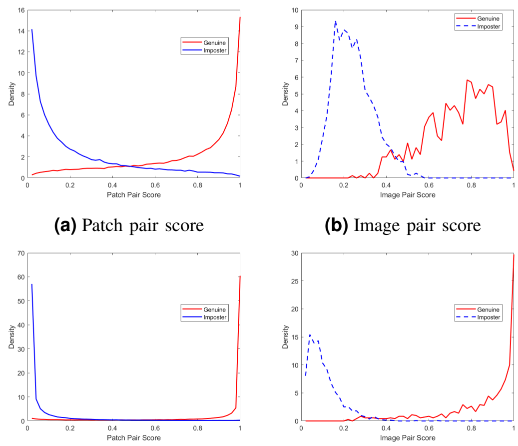


**(a)** Patch pair score **(b)** Image pair score

**(c)** Patch pair score **(d)** Image pair score

Fig. 7: Pair score distributions on UTFVP (a) and (b) 31-pixel, (c) and (d) 82-pixel patches compared

| | EER % | | FRR@FAR=0.1% | |
|---|---|---|---|---|
| Patch Size | Decision | Score | Decision | Score |
| 31-pixel | 3.45 | 4.76 | 18.6 | 13.5 |
| 82-pixel | 1.66 | 2.22 | 9.2 | 8.6 |

TABLE II: Comparison of 31-pixel and 82-pixel patch performances in terms if EER and FRR@FAR=0.1%

On the other hand, Figure 6b does not show any significant trend on SDUMLA-HMT compared to UTFVP. Table III shows that even though 63-pixel patched had the lowest EER, 69-pixel patches performed better in terms of FRR@FAR=0.1%. Figure 8 indicates a better separation between genuine and imposter scores with 69–pixel patch size. Different from UTFVP, some low genuine scores were persistent to change in the patch size while high score genuine were moving to the right edge of the plot. The change in score distribution also improved the verification performance, yet this improvement was not as remarkable as seen in UTFVP. These low score genuine pairs generally had an extreme translation on the object pair. Therefore, the patch size did not help on these pairs alone.

82-pixel and 69-pixel patches were selected as the optimal patch sizes for UTFVP and SDUMLA-HMT, respectively. Further experiments were conducted using these sizes.

| | EER % | | FRR@FAR=0.1% | |
|---|---|---|---|---|
| Patch Size | Decision | Score | Decison | Score |
| 31-pixel | 12.1 | 11.6 | 35.3 | 29.5 |
| 63-pixel | 11.5 | 12.1 | 30.9 | 26.8 |
| 69-pixel | 12.2 | 12.3 | 26.9 | 25.4 |

TABLE III: Comparison of the performance of 31, 63, and 69-pixel patches on SDUMLA-HMT in terms of EER and FRR@FAR=0.1%

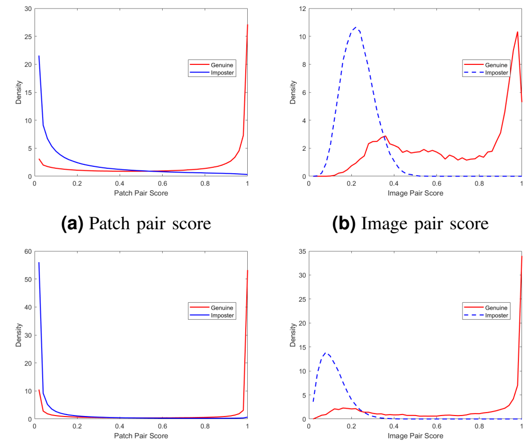


**(a)** Patch pair score **(b)** Image pair score

**(c)** Patch pair score **(d)** Image pair score

Fig. 8: Pair score distributions on SDUMLA-HMT (a) and (b) 31-pixel, (c) and (d) 69-pixel patches compared

### *C. Experiment 2 - Patch Shape*

The purpose of Experiment 2 was to question the square shape patches. Since the veins lay horizontally, rectangular patch shape with different widths were investigated. The height of the patch was determined in the first experiment. The patch widths used in the experiments can be seen in Table I.

| | EER % | | FRR@FAR=0.1% | |
|---|---|---|---|---|
| Patch Width | Decision | Score | Decision | Score |
| 82-pixel | 1.66 | 2.22 | 9.2 | 8.6 |
| 205-pixel | 1.47 | 2.08 | 7.6 | 5.4 |

TABLE IV: Comparison of the performance of 82 and 205 pixels widths on UTFVP in terms of EER and FRR@FAR-0.1%

Figure 9 shows a decrease in EER on both datasets with a rectangular patch shape. The improvement was not as remarkable as seen with the patch size on UTFVP. The UTFVP can be stated as a higher quality dataset. Therefore, a large enough square patch might involve as much information as a rectangular patch. Figure 10 point outs that the rectangular shape provided better separation than the square one. Table IV indicates an increase in the performance with a rectangular shape. Even though the improvement was not remarkable compared to patch size, more horizontal information about the veins helped to solve some ambiguity between genuine and imposter pair.

| | EER % | | FRR@FAR=0.1% | |
|---|---|---|---|---|
| Patch Width | Decision | Score | Decision | Score |
| 69-pixel | 12.2 | 12.3 | 26.9 | 25.4 |
| 174-pixel | 11.3 | 11.3 | 23.9 | 24.3 |

TABLE V: Comparison of the performance of 69 and 174 pixels widths on SDUMLA-HMT in terms of EER and FRR@FAR-0.1%

On the other hand, the improvement was more remarkable on SDUMLA-HMT dataset. Figure 11 indicates that the low genuine score density decreased significantly with the rectangular patch. This led an improvement on the performance of the system, seen in Table V. Horizontal information helped more on SDUMLA-HMT. The translations seen on the dataset might deform the vein structure on vertical axis more than the horizontal one. Therefore, more horizontal information could lead to a better score separation than vertical information.

A small search around the best patch shape was conducted on both datasets. Table VI shows the selected patch shapes for these experiments. The search space was too small to make deductions; however, since a better performing patch shape was found on UTFVP as 87 x 210-pixel, this patch shape was used in further experiments. For SDUMLA-HMT, the selected patch sizes was kept the same as 69 x 174-pixel.

| Dataset | Heights (px) | Widths (px) |
|---|---|---|
| UTFVP | 77, 82, 87 | 200, 205, 210, 215, 220 |
| SDUMLA-HMT | 64, 69, 74 | 169, 174, 179 |

TABLE VI: Search space around the best performing patch shape

### D. Experiment 3 - Overlapping Patches

In this section, two sub-experiments were conducted to investigate the influence of the overlapping patches on training and evaluation stages. In both experiments, the best patch shapes were used. The sizes of the data-sets used in these experiments were proportional to the stride used in each dataset. The stride values for each dataset are given in Table VII.

| Slide(h-w) / Dataset | s0 | s1 | s2 | s3 | s4 |
|---|---|---|---|---|---|
| UTFVP | no-overlap | 53 - 172 | 50 - 103 | 19 - 24 | 16 - 13 |
| SDUMLA-HMT | no-overlap | 42 - 143 | 39 - 85 | 26 - 22 | 12 - 10 |

TABLE VII: Slide values used in overlap experiments for each dataset

*1) Without overlapping Training:* The network was trained by a non-overlapping data-set. This set consisted of 23,930 patch pairs in total. The experiments were conducted on the 5 overlapping settings presented in Table VII

Figure 12a shows a continuous decrease in EER on UTFVP with smaller strides. More overlap on classifiers increases the number of votes; therefore, the performance increased with more overlap. Between *s3* and *s4* evaluation sets, almost no change was observed in EER. After a stride value, the score distribution did not change. Thus, the performance remained the same.

SDUMLA-HMT showed a different trend than UTFVP with smaller strides. Figure 13a indicates an increase in EER after *s1* evaluation set. Larger overlap led a better separation between genuine and imposter scores. However, the low score genuine pairs mentioned on the previous experiments were

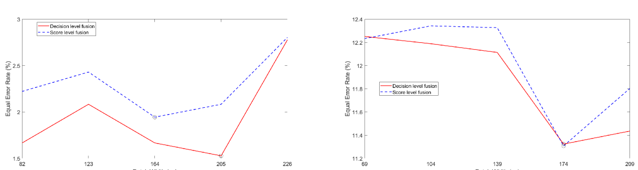


(a) (b)

Fig. 9: EER for varying patch widths (a) UTFVP, (b) SDUMLA-HMT

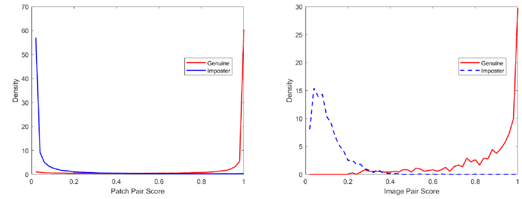


(a) Patch pair score (b) Image pair score

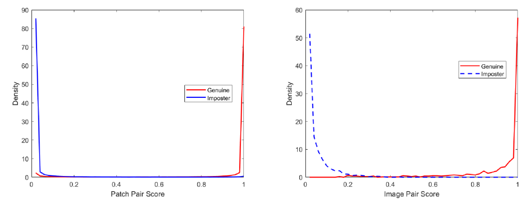


(c) Patch pair score (d) Image pair score

Fig. 10: Pair score distributions on UTFVP (a) and (b) 82-pixel, (c) and (d) 205-pixel patch widths compared

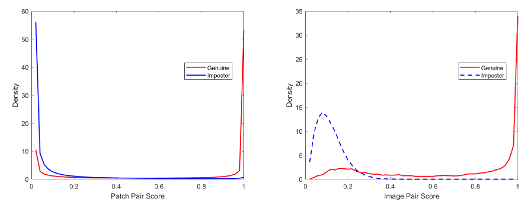


(a) Patch pair score (b) Image pair score

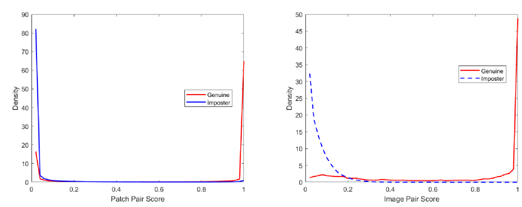


(c) Patch pair score (d) Image pair score

Fig. 11: Pair score distributions on SDUMLA (a) and (b) 69-pixel, (c) and (d) 174-pixel patch widths compared

treated as imposter pairs. Their score also decreased with smaller strides, so the EER increased. Similarly, after a stride, the distribution did not change; therefore, any significant improvement was not observe on the performance.

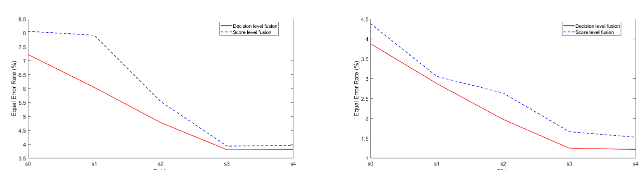


(a) Training with without-overlap (b) Training with overlap

Fig. 12: EER of UTFVP for varying overlap strides. The network trained (a) without-overlap, (b) with overlap

*2) Overlapping Training:* The same experiments were executed using a network trained with an overlapping dataset. *s3* dataset was used for training. It consisted of 952,970 patch pairs, in total.

As seen in the Figure 12b and Figure 13b, the EER was lower with overlapping training. Overlapping applied on the training data helped the network to learn the veins better. Therefore, the network was able to find a better matching. Other than the decrease in EER, the performance of the overlapping classifiers had almost the same trend.

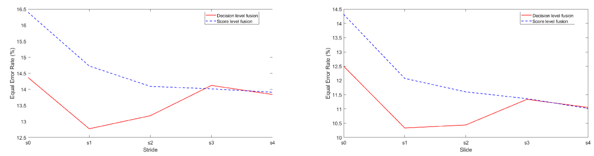

**(a)** Training with without-overlap **(b)** Training with overlap

Fig. 13: EER of SDUMLA-HMT for varying overlap strides. The network trained (a) without overlap, (b) with overlap.

### E. Experiment 4 - Fusion

The aim of this experiment is to demonstrate the feasibility of a non-uniform fusion approach on patch based system. This approach consists of two stages, namely training and evaluation. Therefore, the datasets were divided into two partitions training and evaluation. Training part was used to determine individual thresholds using a set of FAR values. Evaluation set was used to fine tune the individual thresholds at FAR=0.1%. The number of image pairs used in training and evaluation are given in Table VIII.

| | Train | Evaluation |
|---|---|---|
| UTFVP | 7776 | 3044 |
| SDUMLA-HMT | 34560 | 20925 |

TABLE VIII: Number of image pairs involved by train and evaluation sets in Fixed-FAR voting fusion experiments for UTFVP and SDUMLA-HMT

The performance of the fused patch pairs on the evaluation set in terms of FRR@FAR=0.1% as a function of fixed FAR values is seen in Figure 14 for both datasets. Fixed FAR values were selected as 0.215 and 0.145 for UTFVP and SDUMLA-HMT, respectively, since the minimum FRR was reached.

Table IX compares the performance of the proposed FFVF and the current uniform vote fusion methods. A decrease in performance is seen on both dataset with the proposed FFVF. At training stage, the individual thresholds were computed so high so that few genuine patch pairs were able to vote. Moreover, no significant difference between individual patch thresholds was observed.

As the uniform vote fusion outperformed the proposed FFVF approach, further experiments were terminated.

| | UTFVP | | SDUMLA-HMT | |
|---|---|---|---|---|
| | EER% | FRR@FAR=0.1% | EER% | FRR@FAR=0.1% |
| FFVF | 4.53 | 13.6 | 15.3 | 44.4 |
| Uniform Voting Fusion | 3.95 | 18.6 | 12.1 | 35.3 |

TABLE IX: Performance comparison of FFVT and uniform voting fusion methods on both UTFVP and SDUMLA-HMT

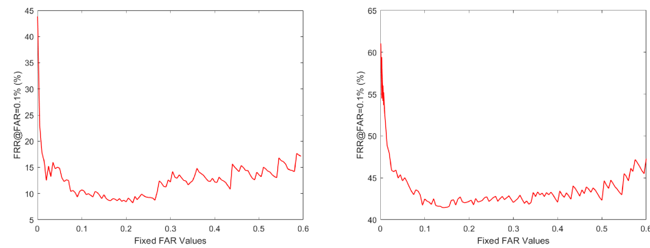


**(a)** UTFVP **(b)** SDUMLA-HMT

Fig. 14: FRR@FAR=0.1% plots (a) UTFVP, (b) SDUMLA-HMT

### F. Experiment 5 - Fine Registration

Two sub-experiments were conducted to optimise the registration step of the patch based approach to finger vein verification.

*1) Local Fine Registration:* Local fine registration assumes that finger vein images are captured with small displacements on the x-axis. Therefore, a small set of shift values up to 4 pixels was experimented.

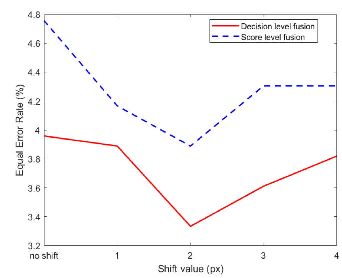


Fig. 15: EER of Local fine registration applied on UTFVP up to 4-pixel shift.

Figure 15 indicates that local fine registration did not provide much improvement on the EER of the system. Even though small improvements were observed, no significant change on the EER was measured. The score distribution graphs presented in Figure 16 compare the difference between no-shift and 4-pixel local shift. After local shift operation, both imposter patch pair and image pair score distribution moved to right significantly. Due to simultaneous increase in both genuine and imposter pair scores, the overall performance of the system did not show an improvement as expected. Therefore, further experiments have been terminated.

*2) Global Fine Registration:* Fine registration was applied on the object whole image. Thus, a larger range for shift values was able to be investigated. The shift operation was applied maximum 40 pixels on both UTFVP and SDUMLA-HMT databases.

As seen in the Figure 17a, lower EER values were observed with larger shift values on UTFVP, approximately 15 - 25 pixels. However, there was a limit for the shift. After approximately 30 pixels, the EER started to increase gradually. This was an expected increase. Because of larger shift values, the object pair image had started to go out of the window, and the location of the finger vein patterns in the image pairs was distorted. At the end, lower matching scores were obtained.

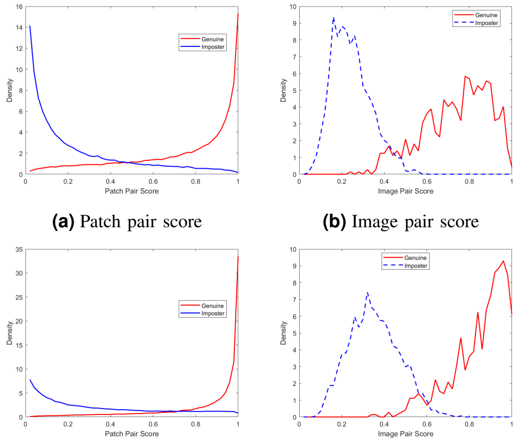


**(a)** Patch pair score **(b)** Image pair score

**(c)** Patch pair score **(d)** Image pair score

Fig. 16: Pair score distribution comparison between (a), (b) no shift and (c), (d) 4-pixel local shift on UTFVP

| | EER % | | FRR@FAR=0.1% | |
|---|---|---|---|---|
| Shift (max.) | Decision | Score | Decision | Score |
| no-shift | 1.22 | 1.53 | 6.9 | 5.4 |
| 18-pixel | 0.3 | 0.4 | 2.4 | 2.1 |

TABLE X: Comparison between coarse registration and 18-pixel global fine registration performances in terms of EER and FRR@FAR=0.1%

Figure 18 compares the score distributions of the best performing patch shape with and without the global fine registration. Table X indicates that global fine registration led to an increase in the performance. This could be interpreted as the global fine registration led a better registration accuracy; therefore the performance improved. Figure 18b and Figure 18d indicate a significant increase in imposter scores with larger shifts; however, different form the local approach, genuine scores increased more than imposters. All patch pairs used in computation of the objective; therefore, even some imposter patch pair scores increases too much, the rest was able to keep the balance.

Figure 17b shows that SDUMLA needs larger shift values for a better registration. This difference between UTFVP and SDUMLA-HMT could be caused by the translations seen on SDUMLA-HMT. Larger shifts would help finding a better match for these pairs.

However, Figure 19e shows a significant distortion in image

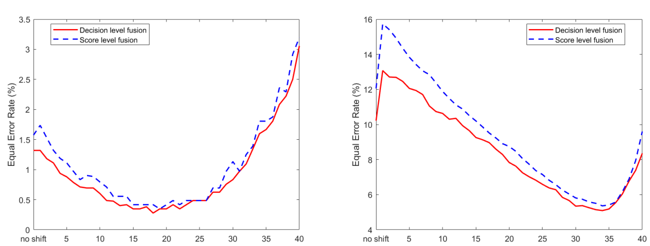


**(a)** UTFVP **(b)** SDUMLA-HMT

Fig. 17: EER of Global fine registration applied on (a) UTFVP, (b) SDUMLA-HMT, up to 40-pixel shift.

| | EER % | | FRR@FAR=0.1% | |
|---|---|---|---|---|
| Shift (max.) | Decision | Score | Decision | Score |
| no-shift | 10.3 | 12.1 | 29.3 | 28.9 |
| 35-pixel | 5.09 | 5.36 | 37.46 | 35.74 |
| 25-pixel | 6.6 | 7.15 | 14.39 | 14.58 |

TABLE XI: Comparison between coarse registration, 35-pixel and 25-pixel global fine registration performances in terms of EER and FRR@FAR=0.1%

pair score distribution compared to Figure 19d. Low score genuine image pair density decreased as expected, yet high scored genuine image pair distribution moved to left. This distortion in genuine pair scores, together with the significant improvement in imposter scores, caused a performance degradation, seen in Table XI.

On the other hand, Table XI also indicates a modest shift around 25-pixel was able to keep the imposter and genuine pair score distribution separated (Figure 19f) while providing a performance improvement .

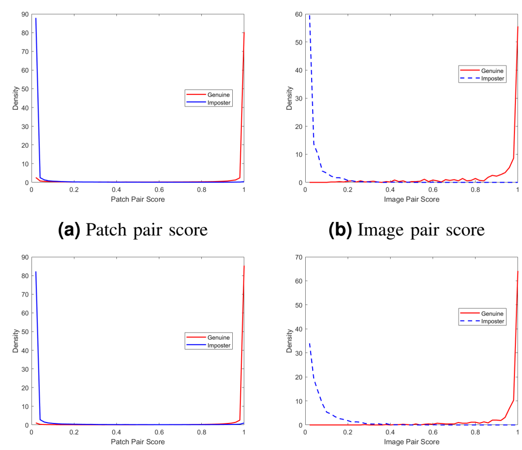


**(a)** Patch pair score **(b)** Image pair score

**(c)** Patch pair score **(d)** Image pair score

Fig. 18: Comparison of score distributions (a),(b) without and (c),(d)with global fine registration on UTFVP. Global fine registration distributions plotted where the EER is lowest(18-pixel shift)

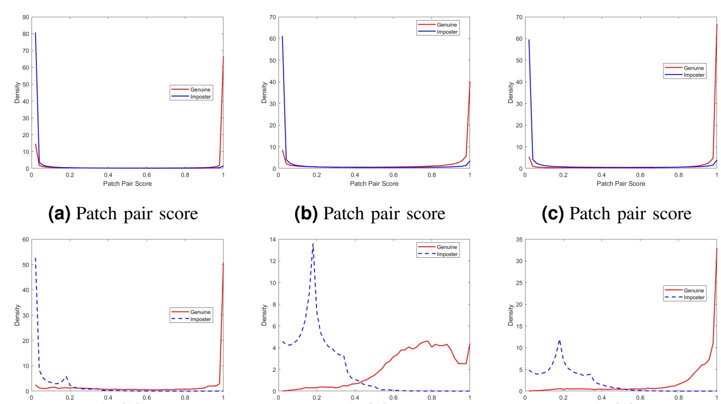


**(a)** Patch pair score **(b)** Patch pair score **(c)** Patch pair score

**(d)** Image pair score **(e)** Image Pair Score **(f)** Image Pair Score

Fig. 19: Comparison of score distributions (a),(d) without and (b),(e)with global fine registration on SDUMLA-HMT. Global fine registration distributions plotted where the EER is lowest(35-pixel shift). c and f shows patch and image score distributions where shift is 25-pixel on SDUMLA-HMT.

## V. Discussion and Future Work

The purpose of this research is to provide an optimisation to the patch-based finger vein verification system. Patch properties, fusion method, and registration step have been tried to be optimised.

Table XII presents some examples of the experiment results in terms of EER in pecentage. Overall, the optimisation achieved promising results with 0.3% of EER on UTFVP. The patch-based finger vein verification system along with the proposed optimisations outperformed some CNN based methods such as [16] (0.42%) and [17] (0.4%). However, the performance is still below conventional methods. For comparison, conventional approaches in [1], [3] have achieved 0.145% and 0.25%, respectively. Yet, the small difference between the obtained and state-of-the-art results indicates the potential of the proposed patch-based system.

Patch size optimisation performed better on UTFVP, while the patch shape was more successful on SDUMLA-HMT. The datasets had some major differences. The image qualities could be considered as high in UTFVP. However, in SDUMLA-HMT, images without visible veins were more common. Moreover, SDUMLA-HMT provided many finger samples with extreme translations causing a deformation in the vein structure. Rectangular patches might avoid these deformations on the vertical axis, while involving the less deformed information on the horizontal axis. As in UTFVP, these translations are not common, a large enough square patch could involve as much information as a rectangular patch.

Overlapping patches improved the performance on both datasets. It has been found that overlapping applied on training data led the network to learn the veins better by adding more variation on training stage. Moreover, overlapping applied on classifiers also improved the performance. As it increases the number of votes for a finger, the more vote generally led a better performance.

Proposed FFVF showed a different behavior than stated in [10] on evaluation stage. Larger fixed FAR values were needed to see a similar trend on FRR@FAR=0.1% graphs.The difference might be caused by the different experimental settings. The FFVF as used in [10] uses individual local patch classifiers and for each of these an optimal threshold is derived, resulting in the same FAR for all local classifiers. For our patch based finger vein recognition, no individual local classifiers were trained, but we did investigate the use of individual local thresholds for the patch classifier, based on the assumption that some areas of the finger vein patterns might have different properties than others. However, this did not result in improved performance as compared to using single threshold for all locations (i.e. the same classifier is used for all patch locations). This is likely due to the fact that local patches between different fingers do not necessarily contain similar features, unlike the facial patches in [10] that contain e.g. the eye, nose or mouth regions.

Fine registration approach was successful in global level. As stated in [13], it is likely to yield a better matching score for imposter pairs. However, the increase in imposter pair scores has been controlled by the mean score used in global fine registration. Even some imposter patch pairs scored high after shifting, the lower scored patches were able to keep this increase in balance since the mean matching score was used in the objective for the global level. On the other hand, because only one patch pair score used as the objective, the increase in imposter scores could not be controlled at local level. Therefore, the increase in imposter pair scores extinguished the improvement on genuine pairs.

In this research, only a few aspects of the patch-based system have been selected for optimisation. In addition to the existing ones, the research arose new research topics.

First of all, some patches could have a little influence on the final score. [20] showed that filtering out the less relevant patches could lead more accurate verification results. Therefore, an algorithm selecting the relevant patches could lead an improvement on the performance.

The implemented Fixed-FAR Voting Fusion revealed that the importance of a patch pair over the others in a finger pair could be ignored. However, some regions could still be more important than the others. For example, joint regions are generally dark and does not involve much visible vein. The implemented fusion method could be adapted to work with regions rather than individual patches. Moreover, such a fusion system could be implemented by defining different weight to different locations on the current decision and score level fusion methods.

The network was out of the scope of this research; however, changes in the CNN could also lead to an improvement. The input size of the network did not change during the patch size and shape experiments. Rather, the extracted larger patch was re-scaled to the input size of the network. This re-scaling operation might deform the vein structure. By changing the input size and the network organisation, better results might be achieved.

Moreover, rather than using the same network, a new network structure could be investigated. Siamese network structures contain two or more identical sub-networks. They are popular among the tasks involving finding similarity or a relationship between two comparable things. Since the weights will be shared among the sub-networks, they tend to have less complexity, therefore less data is needed. In this respect, a Siamese structure might provide more improvement on the patch-based approach.

## VI. Conclusion

In this research, the feasibility of an optimisation on the patch-based finger vein verification system has been investigated. The optimisation has been applied on the patch properties, fusion strategy, and registration approach.

The proposed solutions achieved promising results with 0.3% of EER and 0.999 AUC on UTFVP, and 6.6% of EER anf 0.969 AUC on SDUMLA-HMT.

| | | UTFVP | | | | SDUMLA-HMT | | | |
|---|---|---|---|---|---|---|---|---|---|
| | | Before | | After | | Before | | After | |
| | | Decision | Score | Decision | Score | Decison | Score | Decison | Score |
| Patch Properties | Size | 3.95% | 4.76% | 1.66% | 2.22% | 12.1 | 11.6% | 12.2% | 12.3% |
| | Size+Shape | 1.66 | 2.22% | 1.53% | 2.08% | 12.2% | 0.123% | 0.113% | 11.3% |
| | Size+Shape+Overall | 1.53% | 2.08% | 1.22% | 1.53% | 11.3% | 11.3% | 10.3% | 12.1% |
| Fine Registration | Local | 3.95% | 4.76% | 3.33% | 3.88% | - | - | - | - |
| | Patch Properties+ Global | 1.2% | 1.53% | 0.3% | 0.4% | 10.3% | 12.1% | 6.6% | 7.15% |
| Overall | | 3.95% | 4.76% | 0.3% | 0.4% | 12.1% | 11.6% | 6.6% | 7.15% |

TABLE XII: Overall comparison of the experiments

Optimal patch properties are dependent on the dataset characteristics. On an input data having extreme translations, rectangle patches could lead better results than square ones.

Overlapping helped at both training and evaluation stages on both datasets. When it is applied on the training data, overlapping leads better learning. Overlapping on the classifiers improves the performance by increasing the number of votes per image pair.

Contrary to the expected, differences between individual patches could be ignored because the difference between computed thresholds were negligible. Moreover, local patches extracted from different finger pairs were not necessarily to have similar features. Setting and fine tuning one threshold for all patches have performed better than individual thresholds on both datasets.

The matching score based fine registration approach led to a better registration accuracy on global level. Local level approach did not perform as expected due to the uncontrolled increase in imposter pair scores.

Overall, the proposed optimisations achieved promising results and reinforced the potential of the patch-based finger vein verification approach. Even though the obtained results are less satisfied than the state-of-the-art, any improvements made on these approaches proposed in this research may achieve more satisfied results.

## REFERENCES


[1] N. Miura, A. Nagasaka, T. Miyatake, Feature extraction of finger-vein patterns based on repeated line tracking and its application to personal identification,T. Machine Vision and Applications, October 2004, Vol. 15, pp. 194-203.

[2] N. Miura, A. Nagasaka, T. Miyatake,Extraction of Finger-Vein Patterns Using Maximum Curvature Points in Image Profiles, IEICE TRANSACTIONS on Information and Systems, August 2007, Vol. E90-D, pp. 1185-119.

[3] W. Song, T. Kim, H. C. Kim, J. H, Choi, H. J. Kong, S. R. Lee, A finger-vein verification system using mean curvature, Pattern Recognition Letters, August 2011, vol. 32, pp. 1541-1547.

[4] J. Peng, N. Wang, A. A. El-Latif, Q. Li, X. Niu, Finger-vein Verification Using Gabor Filter and SIFT Feature Matching, International Conference on Intelligent Information Hiding and Multimedia Signal Processing, July 2012.

[5] B. A. Rosdi, C. W. Shing, S. A. Suandi, Finger Vein Recognition Using Local Line Binary Pattern, 2011, Sensors, vol. 11, pp. 11357-11371.

[6] X. Meng, X. Xi, G. Yang, Y. Yin, Finger vein recognition based on deformation information, Science China Information Sciences, May 2018.

[7] H. Qin, L Qin, L. Xue, C. Yu, X. Liang, Finger-Vein Verification Based on Multi-Features Fusion, Sensors, 2013, vol. 13, pp. 15048-15067.

[8] A. Radzi, M. K. Hani, R. Bakhteri, Finger-vein biometric identification using convolutional neural network, Turkish Journal of Electrical Engineering and Computer Sciences, 2016, vol. 24, pp. 1863 1878.

[9] B. T. Ton and R. N. J. Veldhuis, A high quality finger vascular pattern dataset collected using a custom designed capturing device, International Conference on Biometrics (ICB), 2013, pp. 1 - 5.

[10] L. Spreeuwers, and R. N. J. Veldhuis, S. Sultanali,J. Diephuis, Fixed FAR vote fusion of regional facial classifiers, International Conference of the Biometrics Special Interest Group (BIOSIG), 2014, pp. 1 - 4.

[11] S. de Boer, Patch-based Finger Vein Verification with Convolutional Neural Network, 2017.

[12] Paul J Besl, Neil D McKay, et al. A method for registration of 3-d shapes. IEEE Transactions on pattern analysis and machine intelligence, 1992, vol. 14(2), pp. 239 - 256.

[13] L. Spreeuwers, B. Boom, Better than best:Matching score based face registration, 2007.

[14] G. Meng, P. Fang, B. Znag, Finger Vein Recognition Based on Convolutional Neural Network, MATEC Web Conference, 2017, vol. 128.

[15] W. Liu, W. Li, L. Sun, L. Zhang, P. Cheng, Finger vein recognition based on deep learning, IEEE Conference on Industrial Electronics and Applications (ICIEA), 2017.

[16] H. Huang, S. Liu, H. Zeng, L. Ni, Y. Zang, W. Li, DeepVein: Novel finger vein verification methods based on Deep Convolutional Neural Networks, 2017, Security and Behavior Analysis (ISBA).

[17] H. G. Hong, M. B. Lee, K. R. Park, Convolutional Neural Network-Based Finger-Vein Recognition Using NIR Image Sensors, Sensors, 2017.

[18] A. Krizhevsky, N. Vinod, H. Geoffrey Hinton, The CIFAR-10 dataset, 2014, online: http://www.cs.toronto.edu/kriz/cifar

[19] J. Deng, W. Dong, R. Socher, L.J. Li, K. Li, L. Fei-Fei, Imagenet: A large-scale hierarchical image database, Computer Vision and Pattern Recognition(CVPR), June 2009, pp. 248-255.

[20] L. Hou, D. Samaras, T. M. Kurc, Y. Gao, Patch Based Convolutional Neural Network for Whole Slide Tissue Image Clssification, IEEE Computer Society Conference on Computer Vision and Pattern Recognition. 2016, 2424 - 2433.

[21] G. Keren, J. Deng, J. Pohjalinan, B.W. Schuller, Convolutional Neural Network with Data Augmentation for Classifying Speakers' Native Language , Interspeech, 2016.

[22] S. Hoffman, R. Sharma, A. Ross, Convolutional Neural Network for Iris Presentation Attack Detection: Toward Cross-Dataset and Cross-Sensor Generalisation, 2018.

[23] B. Huang, Y. Dai, R. Li, D. tang, W. Li, Finger Vein Authentication based on Wide Line Detector and Pattern Normalisation, International Conference on Pattern Recognition, 2010.

[24] E.C. Lee, H. Jung, D. Kim, New Finger Vein Biometrics using Near Infrared Imaging, 2011, Sensors, vol. 11.

[25] JD. Wu, LT. Lui, Finger Vein Identification Using Principal Component Analysis and the Neural Network Technique, 2011, Expert Systems with Applications, Vol. 38, pp. 5423 - 5427.

[26] JD. Wu, LT. Liu, Finger Vein Identification using SVM and Neural Network Technique, 2011, Expert Systems with Applications, Vol. 38, pp. 14284 - 14289

[27] Y. Yin, L. Liu, X. Sun, SDUMLA-HMT: A Multimodal Biometric Database, Chinese Conference on Biometric Recognition (CCBR), 2011, LNCS 7098, pp. 260-268.

[28] C.B. Yu, H.F. Qin, Y.Z. Cui, X.Q. Hu, Finger-vein image recognition combining modified hausdorff distance with minutiae feature matching, 2009, Interdisciplinary Sciences: Computational Life Sciences, Vol. 1, pp. 280 - 289.

[29] F.Liu, G. Yang, Y. Yin, S. Wang, Singular value decomposition based minutiae matching method for finger vein recognition, Neurocomputing, 2014, Vol. 145, pp. 75 - 89.

[30] P. Wang, L.C. Tran, Q.Ji, Improving Face Recognition by Online Image Alignment, International Conference on Pattern Recognition (ICPR'06), 2006, pp. 311 - 314.
[31] A. Kortylewski, A. Schneider,T. Gerig, B. Egger, A. Morel-Forster, T. Vetter, Thomas,Training Deep Face Recognition Systems with Synthetic Data, 2018.
[32] L. Perez, J. Wang, Jason, The effectiveness of data augmentation in image classification using deep learning, 2017.
[33] L. Dong, G. Yang, Y. Yin, F Liu, X Xi, Finger vein verification based on a personalized best patches map, Biometrics (IJCB), 2014, pp. 1 - 8.
[34] H. Qin, L. Qin, L. Xue, X. He, C. Yu, X. Liang, Finger-vein verification based on multi-features fusion, Sensors, 2013, vol. 13, pp. 15048 - 15067.
[35] H. Qin, M. El-Yacoubi, Deep representation-based feature extraction and recovering for finger-vein verification, IEEE Transactions on Information Forensics and Security, 2017, vol. 12, pp. 1816 - 1829.
[36] P. Zhu, L. Zhang, Q. Hu, S.C.K. Shiu, Multi-scale patch based collaborative representation for face recognition with margin distribution optimization, European Conference on Computer Vision, 2012, 822 - 835.
[37] F. Liu, Y. Yin, G. Yang, L. Dong, X. Xi, Finger vein recognition with superpixel-based features,Biometrics (IJCB), 2014 IEEE International Joint Conference on, 2014, 1 - 8.